Proceedings of the 9th WSEAS International Conference on Applied Mathematics, Istanbul, Turkey, May 27-29, 2006 (pp572-579)

Numerical Modeling of Seawater Intrusion in Coastal Aquifer Using Finite Volume Unstructured Mesh Method

MEHDI HAMIDI, SAEED REZA SABBAGH YAZDI
M.Sc. of Hydraulic Structures, Assistant Professor
Department of Civil Engineering
KN Toosi University of Technology, Tehran
1346, Vali Asr Street, Tehran
IRAN

Abstract: - Saltwater intrusion widely occurs in coastal areas. Therefore, dissolved salts are the most common contaminants in freshwater in coastal aquifers and this contamination arises from saltwater invasion, caused primarily by human activities due to heavy urbanization. For investigation of the methods of increasing storage of fresh ground water and prevention of seawater encroachment, predicting the location and movement of the saltwater interface is crucial. Saltwater intrusion problems are so complex and generally cannot be analytically solved. Hence, numerical methods are ideal tools for the simulation and prediction of results.

In this paper, a two-dimensional finite volume unstructured mesh method (FVUM) based on a triangular mesh is developed for analyzing the evolution of the saltwater intrusion into coastal aquifer systems. The model formulation consists of a ground-water flow equation and a salt transport equation. Simulation results are compared with previously published solutions where good agreement is observed.

Key-Words: - Saltwater Intrusion, Coastal Aquifer, Dispersion, Unstructured Finite Volume, Vertex-Centered

1 Introduction

The seawater intrusion in coastal aquifer has long been widely attracting an attention of researchers for the management of coastal water resource and environment protection. It is worthwhile note that human water-use patterns are the most important factors for seawater intrusion. Seawater encroachment obviously limits the usage of groundwater for domestic, agricultural, or industrial purposes. Hence, there is a need to predict the location and movement of the possible danger of contamination fronts. Practical management requires knowledge of not only the present response, but also of the long-term transient response. For these managerial purposes, a numerical model can assist in estimating the location of the freshwater/saltwater interface for given sets of hydrological conditions.

In the past, several numerical models have been proposed to simulate the problem of saltwater intrusion into aquifers. As early as 1964, Henry [1964] developed the first analytical solution for the steady-state salt distribution in a confined coastal aquifer. In many cases, however, a steady-state solution for transient simulations was not obtained due to the high computing costs. Segol, Pinder and Gray [1975] developed the first transient solution based on a velocity-dependent dispersion coefficient using the Galerkin finite element method to solve the set of non-linear partial differential equations describing the movement of a saltwater front in a coastal confined aquifer. Numerous other researchers, such as Frind [1982], Huyakorn, Andersen, Mercer, Harold and White [1987], Voss [1984] and Cheng, Strobl, Yeh, Lin and Choi [1998] have implemented numerical models for simulating saltwater intrusion problems using a variety of different methods.

The problem of saltwater intrusion into coastal aquifers can be formulated in terms of two tightly coupled, non-linear partial differential equations. The first equation describes the flow of a variable-density fluid, and the second equation describes the transport of dissolved salt. Due to the inherently complex boundary conditions and intricate physical geometries in any practical problem, an analytical solution is not possible. This paper presents a finite volume unstructured mesh method (FVUM) for modeling saltwater intrusion into aquifer systems. The solution domain is tessellated with triangles and the control volumes are constructed around the triangle vertices. Using this strategy the coupled partial differential conservation equations are discretised into a system of differential/algebraic equations. These equations are then resolved in time.

These methods are suitable for intricate physical geometries and density-dependent flow and transport through saturated-unsaturated porous media. Simulation results for two cases of confined and unconfined aquifer are presented and compared with previously published solutions to assess the performance of the newly proposed computational model.

2 Problem Formulation

The problem of seawater intrusion into aquifers is governed by a coupled nonlinear system of two partial differential equations. The first differential equation is the flow equation that describes the head distribution in the aquifer of interest. The classically used pressure head variable employed in the flow equation has been replaced by the use of an equivalent freshwater head that generally results in the elimination of static quantities and improves numerical efficiency.

The flow equation for a confined aquifer can be written as [Frind, 1982; Huyakorn et al., 1987]:

$$S_s \frac{\partial h}{\partial t} = \nabla.\left[K\left(\nabla h + \eta C \nabla z\right)\right] \quad (1)$$

Where h is the reference hydraulic head referred to as the freshwater head; K is the hydraulic conductivity tensor; η is the density coupling coefficient; C is the solute concentration; S_s is the specific storage; t is time; z is elevation.

The reference head and the density coupling coefficient in (1) are defined as

$$h = \frac{p}{\rho_0 g} + z \quad (2)$$

$$\eta = \frac{\varepsilon}{C_{\max}} \quad (3)$$

Where P is the fluid pressure; g is the gravitational acceleration; $C_{\max}$ is the concentration that corresponds to the maximum density $\rho_{\max}$; ρ_o is the reference (freshwater) density; ε is the density difference ratio defined as

$$\varepsilon = \frac{\rho_{\max}}{\rho_0} - 1 \quad (4)$$

ρ is the density of the mixed fluid (fresh water and saltwater) and the relationship between fluid density and concentration under isothermal conditions is expressed as:

$$\rho = \rho_0(1 + \eta C) = \rho_0(1 + \rho_r) \quad (5)$$

Where ρ_r is the relative density.

The other differential equation is the transport (dispersion) equation, which is used to describe the chemical concentration. To describe salt transport, we use the following form of the advective-dispersive equation:

$$n\frac{\partial C}{\partial t} = \nabla.\left(nD\nabla C\right) - \nabla.\left(CV\right) \quad (6)$$

Where n is porosity and D is the dispersion tensor, whose terms, according to Bear [1979], are defined in a two-dimensional x - z coordinate system as:

$$D_{xx} = \alpha_L \frac{v_x^2}{|v|} + \alpha_T \frac{v_z^2}{|v|} + \tau D_m \quad (7)$$

$$D_{zz} = \alpha_T \frac{v_x^2}{|v|} + \alpha_L \frac{v_z^2}{|v|} + \tau D_m \quad (8)$$

$$D_{xz} = D_{zx} = \left(\alpha_L - \alpha_T\right)\frac{v_x v_z}{|v|} \quad (9)$$

Where α_L and α_T are the longitudinal and transverse dispersivities respectively, D_m is the molecular diffusion coefficient, and τ is tortuosity. The Darcy velocity vector and linear velocity can be expressed as

$$V = -K\left(\nabla h + \eta C \nabla z\right) \quad (10)$$

$$v = V / n \quad (11)$$

To obtain a unique solution to (1) and (6), initial and boundary conditions must be specified.

For the flow equation, the initial condition may be expressed as

$$h(x, z; 0) = h_0(x, z) \text{ In } R \quad (12)$$

Where R is region of interest; h_0 is the initial head.

The boundary conditions may be stated as follows.

Dirichlet boundary condition:

$$h(x_b, z_b; t) = h_d(x, z; t) \quad \text{In } B_d \quad (13)$$

Neumann boundary condition:

$$V.n_i = V_n(x_b, z_b; t) \text{ In } B_n \quad (14)$$

where n_i is the outward unit vector normal to the boundary; (x_b, z_b) is a spatial coordinate on the boundary; h_d and V_n are the Dirichlet functional value and Neumann flux, respectively.

For the transport equation, the initial condition may be expressed as

$$C(x, z; 0) = C_0(x, z) \text{ In } R \quad (15)$$

The boundary conditions may be stated as follows.

Dirichlet boundary condition:

$$C(x_b, z_b; t) = C_d(x_b, z_b; t) \quad \text{In} \quad B_d \tag{16}$$

Neumann boundary condition:

$$n_i.(-nD\nabla C) = V_n(x_b, z_b; t) \quad \text{In} \quad B_n \tag{17}$$

Cauchy boundary conditions:

$$n_i.(CV - nD\nabla C) = V_c(x_b, z_b; t) \quad \text{In} \quad B_c \tag{18}$$

Where C_d, V_n and V_c are the Dirichlet functional value, Neumann flux and Cauchy flux, respectively.

3 Problem Solution

During the last twenty years there has been a strong focus upon the utilization of the Finite Volume (FV) or Control Volume (CV) approaches for solving fluid flow and heat transfer problems or, as it is more generally known, problems in Computational Fluid Dynamics (CFD). This success is mostly due to the conservative nature of the scheme and the fact that the terms appearing in the resulting algebraic equations have a specific physical interpretation. In fact, the straightforward formulation and low computational cost compared with other methods have made CV the preferred choice for most CFD practitioners. Over the last ten years, several control volume based-unstructured mesh (FVUM) approaches have in many way overcome the structured nature of the original control volume method.

In general, the FVUM methods can be categorized into two approaches, namely, vertex-centered or cell-centered. The classification of the approach is based on the relationship between the control volume and the finite element like unstructured mesh. The approach described here is the vertex-centered, which is more generally known as the Control Volume based Finite Element Mesh method. In a discrete solution procedure, the solution domain is subdivided into smaller regions and nodes are distributed throughout the domain, the connections between the nodes and the sub-regions are known as a mesh. In a finite element mesh, the sub-regions are called elements, with the vertices of the elements being the nodal locations. For the vertex centered approach only the basic elements, which triangles with three nodes are considered.

In the solution domain, each node is associated with one control volume. Each surface of the control volume is defined as the vector that joins the centroid of an element to the centroid of the adjacent one as shown in Figure 1. Consequently, each of the triangular elements is divided into three by these control surfaces (CS). Each control volume consist of some triangular shapes, called sub-control volumes (SCV) and are illustrated in Figure 2. Thus, a control volume consists of the sum of all neighboring SCVs that surround any given node. The CV is polygonal in shape and can be assembled in a straightforward and efficient manner at the element level. The flow across each control surface must be determined by an integral. The FVUM discretisation process is initiated by utilizing the integrated form of the equation. (1) and (6). Integrating the flow equation (1) and the transport equation (6) over an arbitrary control volume yields:

$$\int_v S_s \frac{\partial h}{\partial t} dv = \int_v \nabla.[K(\nabla h + \eta C \nabla z)] dv \tag{16}$$

$$\int_v n \frac{\partial C}{\partial t} dv = \int_v \nabla.(nD\nabla C) dv - \int_v \nabla.(CV) dv \tag{17}$$

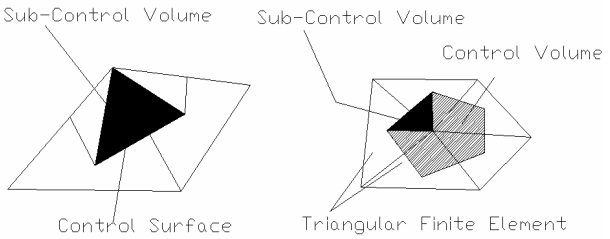

Figure 1: Construction of a control volume from triangular finite element and sub-control volumes

Applying the Gauss divergence theorem to the right-hand side of equation (16), (17) and using a lumped mass approach for the time derivative term gives

$$S_p \frac{\partial h_p}{\partial t} v_p = \int_s [K(\nabla h + \eta C \nabla z)].dn \tag{18}$$

$$n \frac{\partial C_p}{\partial t} v_p = \int_s (nD\nabla C).dn - \int_s (CV).dn \tag{19}$$

Where dn represents the components of the outward normal surface vector to the control surface S and an anticlockwise traversal of the finite volume integration is assumed, i.e., dn can be approximated in the discrete sense by $dn = \Delta z\vec{i} - \Delta x\vec{k}$; Δx and Δz represent the x and z components of the SCV face; v_p is the area of the control volume, and is evaluated for the vertex case as

$$v_p = \sum_{i=1}^{N_{pscv}} v_{scv_i} \tag{20}$$

where, N_{pscv} is the total number of SCV's that make up the control volume associated with the node p .

The integrals in equations (18) and (19) are line integrals. These integrals will be approximated by the midpoint approximation for each control surface. To effect this midpoint approximation, the argument of the integrals is required at the midpoint of the control surface and it is for these surfaces that the outward normal vector will be required. The integral in equation (18) can be rewritten as

$$\int_s [K(\nabla h + \eta C \nabla z)].dn$$

$$= \sum_{i=1}^{N_{pscv}} K^j \left(\left(\frac{\partial h^j}{\partial x} \right) i + \left(\frac{\partial h^j}{\partial z} + \eta C^j \right) k \right).\left(\Delta z^j i - \Delta x^j k \right)$$

$$= \sum_{i=1}^{N_{pscv}} \left(K_x^j \frac{\partial h^j}{\partial x} \Delta z^j - K_z^j \left(\frac{\partial h^j}{\partial z} + \eta C^j \right) \Delta x^j \right) \quad (21)$$

Using the Gauss Divergence theorem, $\frac{\partial h}{\partial x}$ and $\frac{\partial h}{\partial z}$ in center of each element is written:

$$\frac{\partial h}{\partial x} = \frac{1}{\Omega_{e.e}} \sum_{i=1}^{3} \bar{h}_i \Delta z \qquad \frac{\partial h}{\partial z} = -\frac{1}{\Omega_{e.e}} \sum_{i=1}^{3} \bar{h}_i \Delta x \quad (22)$$

Where $\Omega_{e.e}$ represents the area of each element. C in center of each element is evaluated with:

$$C = \frac{1}{3} \sum_{i=1}^{3} C_i \quad (23)$$

The first integral of the right hand side in equation (19) can be rewritten as

$$\int_s (nD\nabla C).dn = n \sum_{i=1}^{N_{pscv}} [D^j \nabla C^j].dn$$

$$= n \sum_{i=1}^{N_{pscv}} \left[\left(D_{xx}^j \frac{\partial C^j}{\partial x} + D_{xz}^j \frac{\partial C^j}{\partial z} \right) \Delta z^j - \left(D_{xz}^j \frac{\partial C^j}{\partial x} + D_{zz}^j \frac{\partial C^j}{\partial z} \right) \Delta x^j \right] \quad (24)$$

The second integral of the right hand side in equation (19) can be rewritten as:

$$\int_s (CV).dn = -\int_s [CK(\nabla h + \eta C \nabla z)].dn$$

$$= -\sum_{j=1}^{N_{pscv}} C^j \left[K(\nabla h^j + \eta C^j \nabla z^j) \right].dn$$

$$= -\sum_{i=1}^{N_{pscv}} C^j \left(K_x^j \frac{\partial h^j}{\partial x} \Delta z^j - K_z^j \left(\frac{\partial h^j}{\partial z} + \eta C^j \right) \Delta x^j \right) \quad (25)$$

Using the Gauss Divergence theorem $\frac{\partial C}{\partial x}$ and $\frac{\partial C}{\partial z}$ in center of each element are:

$$\frac{\partial C}{\partial x} = \frac{1}{\Omega_{e.e}} \sum_{i=1}^{3} \bar{C}_i \Delta z \;,\; \frac{\partial C}{\partial z} = -\frac{1}{\Omega_{e.e}} \sum_{i=1}^{3} \bar{C}_i \Delta x \quad (26)$$

The components of the dispersion tensor will be approximated as

$$D_{xx} = \alpha_L \frac{v_x^2}{|v|} + \alpha_T \frac{v_z^2}{|v|} + D_m \tau \quad (27)$$

$$D_{zz} = \alpha_T \frac{v_x^2}{|v|} + \alpha_L \frac{v_z^2}{|v|} + D_m \tau \quad (28)$$

$$D_{xz} = D_{zx} = (\alpha_L - \alpha_T) \frac{v_x v_z}{|v|} \quad (29)$$

where

$$V_x = -K_x \frac{\partial h}{\partial x} \;,\; V_z = -K_z \left(\frac{\partial h}{\partial z} + \eta C \right) \quad (30)$$

$$v = \frac{V}{n} \;,\; |v| = \sqrt{v_x^2 + v_z^2} \quad (31)$$

In order to stablizing the numerical solution, time step is restricted by:

$$\Delta t = \left(S_s \Omega_n \Big/ \max(k_{xx}, k_{zz}) \right)_{\min} \quad (32)$$

Where Ω_n is area of each control volume and k_{xx} and k_{zz} are hydraulic conductivity in x and z direction.

In order to solve the resulted ordinary differential equations, the boundary conditions must be treated numerically. After assembling the nodal control volume equations, complete conservation equations will exist for all interior control volumes.

However, at solution boundaries, the corresponding control volume will have two control surfaces for which boundary conditions must be applied to complete the equations for conservation. Figure 2 illustrates sub-control volumes for a triangular element where two of its sides form part of the solution domain boundary. For evaluation of boundary conditions along these sides it is necessary to integrate the corresponding boundary control surfaces (BCS) as shown in Figure 2.

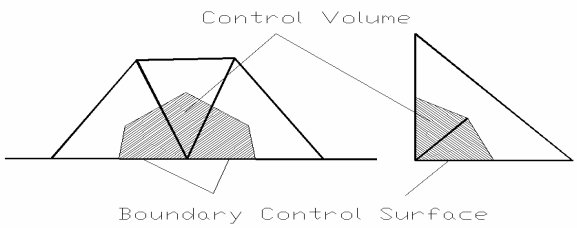

Figure 2: Boundary element, boundary control surface and boundary control volume

4 Numerical Simulation

To verify the above described numerical model, two examples are considered, for which numerical modeling results are available. These examples describe density-dependent flow and transport

through porous media in confined and unconfined aquifer which can be used for verification of our numerical model.

4.1 Confined Aquifer simulation

This example concerns groundwater flow and salt transport in a coastal confined aquifer. This example is known as Henry [1959] problem which is described schematically in Figure 2. The transient analyses were performed. The parameters were chosen so that the analyzed cases correspond to those numerically solved by other researchers. The boundary conditions employed in present numerical simulation are also shown. in Figure 3.

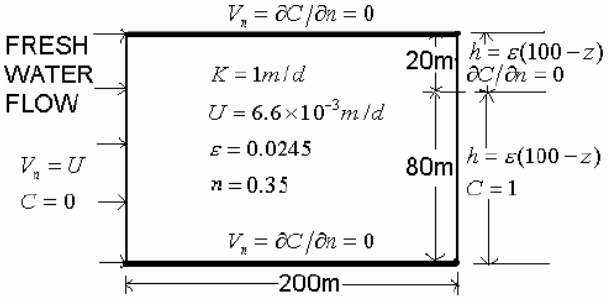

Figure 3: Problem description of saltwater intrusion in a coastal confined aquifer [9]

The aquifer under consideration is a uniform isotropic aquifer that is bounded below and above by impermeable strata. In addition, the aquifer is exposed on the right side by a stationary saltwater body and is recharged on the left side by a constant freshwater influx. The coastal boundary condition allows convective mass transport out of the system over the top portion $(80m \le z \le 100m)$. Thereupon, the normal concentration gradient is set equal to zero. The initial concentration and reference hydraulic head were set to zero.

The aquifer region is represented by a two-dimensional triangular unstructured mesh consisting of 842 triangular elements and 482 nodes as shown in Figure 4.

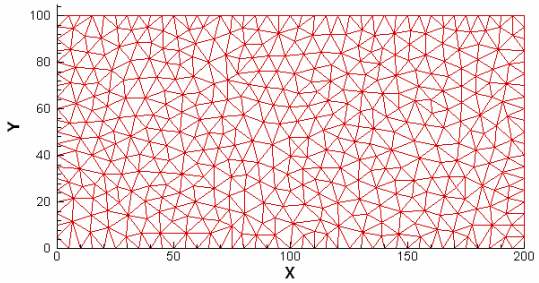

Figure 4: A two-dimensional unstructured mesh of coastal confined aquifer

Two cases of variable dispersion and constant coefficients were selected.

For the variable dispersion case, D_m was set to zero and the longitudinal and transverse dispersivities α_L and α_T were set to 3.5m.

Figure 5 shows the 0.5-isochlor distributions using FVUM for the steady state. It is apparent from Figure 5 that the present analyses are in good agreement with those of Cheng et.al [1998], Huyakorn et al. [1987] and Frind. [1982].

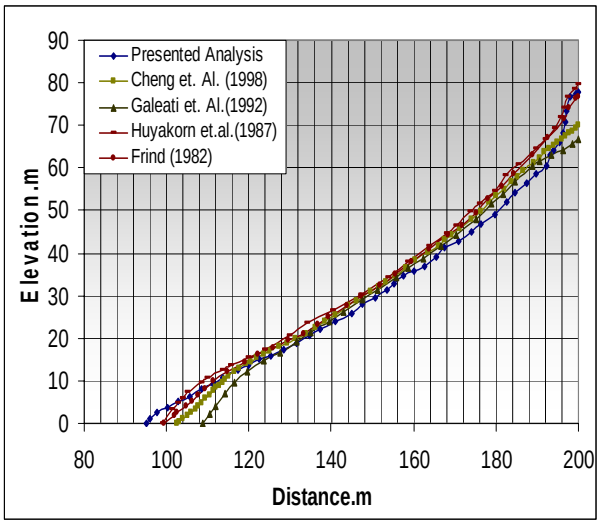

Figure 5: The 0.5-isochlor distribution for steady state, variable dispersion case

Salt concentration distribution and head distribution in variable dispersion case are shown in Figure 6 and 7.

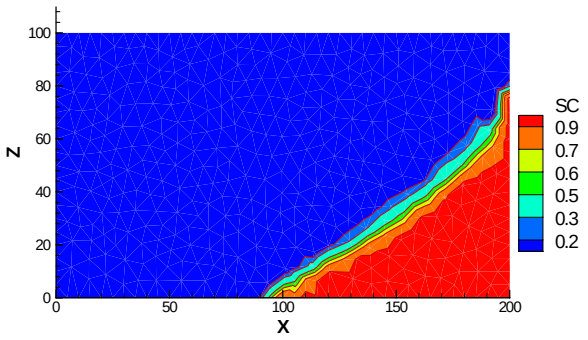

Figure 6: Salt concentration distribution, for steady state, variable dispersion case

For the constant dispersion case, the molecular diffusion coefficient D_m was set equal to $6.6*10^{-2}\,m^2/d$, and α_L and α_T were set to zero.

Figure 8 shows the 0.5-isochlor distributions using FVUM for the transient state at t=6000 days for the constant dispersion case. It can be observed from these figures that the results are in satisfactory

agreement with previously published solutions [Huyakorn et al., 1987; Frind, 1982; Cheng et al., 1998 and Liu et al.2001].

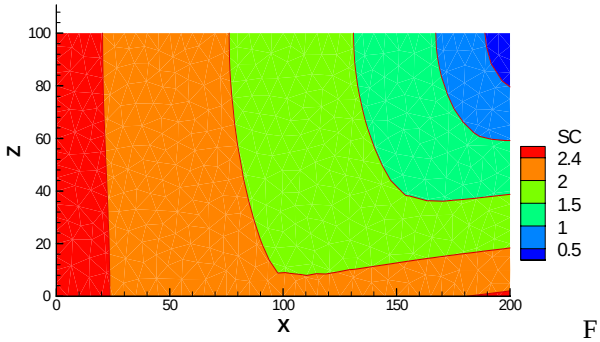

Figure 7 : Head distribution, for steady state, variable dispersion case

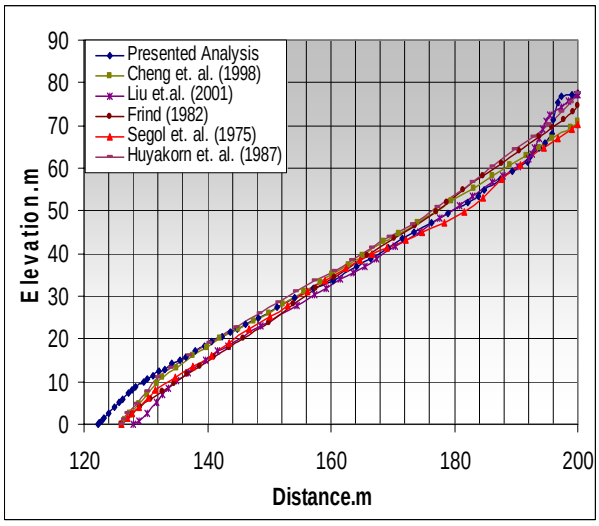

Figure 8: The 0.5-isochlors distribution for transient state at t=6000 days, constant dispersion case

Salt concentration distribution and head distribution in constant dispersion case are shown in Figure 9 and 10.

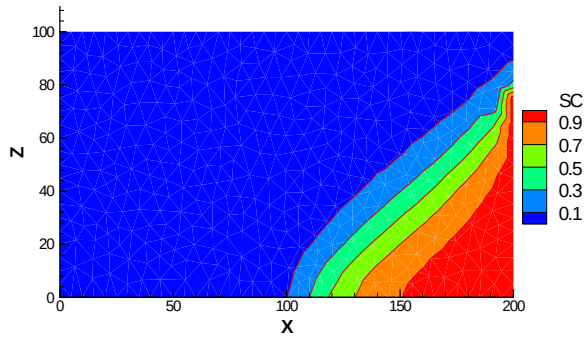

Figure 9: Salt concentration distribution for transient state at t=6000 days, constant dispersion case

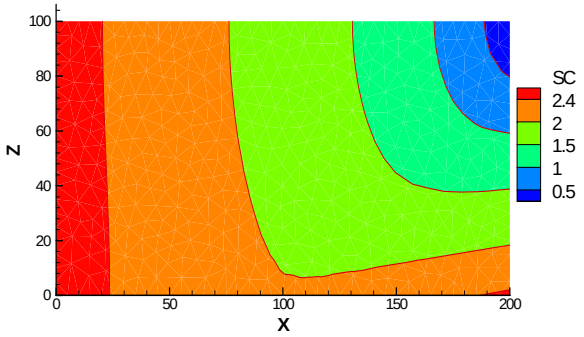

Figure 10: Head distribution for transient state at t=6000 days, constant dispersion case

4.1 Unconfined Aquifer simulation

This example involves an anisotropic unconfined aquifer that is recharged by freshwater from top and from landward side and invaded by saltwater on the coastal side. The saturated thickness is assumed to be 50 m. In addition, the top boundary of pheriatic aquifer, which is free surface, is assumed to be fixed at an elevation of 50 m above the base of aquifer. Although this approximate assumption of the free surface conditions may seem unreasonable at first glance, it can be considered a conceivable assumption for this particular problem because the maximum rise in the water table because of recharge is not expected to exceed but a few percent of initial saturated thickness of 50 m (Huyakorn et al. 1987).

This unconfined aquifer is schematically shown, in Figure 11. The steady-state analyses were performed. The parameters were chosen so that the cases analyzed correspond to those solved numerically by other researchers. The boundary conditions employed in presented numerical simulation are also shown in Figure 11.

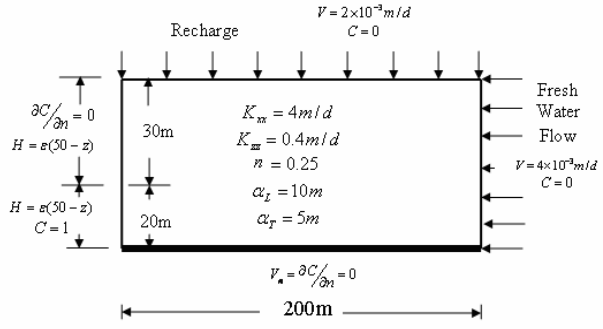

Figure 11: Problem description of saltwater intrusion in a coastal unconfined aquifer [2]

The initial concentration and reference hydraulic head were set to zero.

The aquifer region was represented by a two-dimensional triangular unstructured mesh consisting

of 265 triangular elements and 428 nodes as shown in Figure 12.

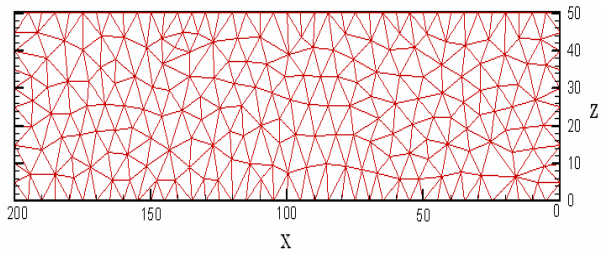

Figure 12: A two-dimensional unstructured mesh of coastal unconfined aquifer

For steady-state analysis, the longitudinal and transverse dispersivities α_L and α_T were set to 10m and 5m.

Figure 13 shows the 0.5-isochlor distributions using FVUM for the steady state. It is apparent from Figure 13 that the present analyses are in good agreement with those of Cheng et.al [1998], Galeati et al. [1987].

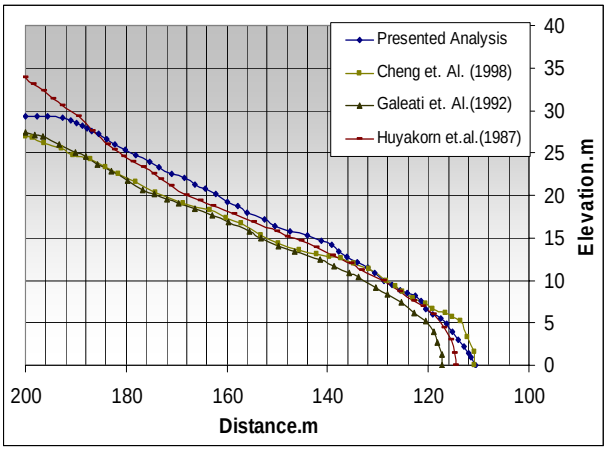

Figure 13: The 0.5-isochlor distribution for steady-state in unconfined coastal aquifer

Salt concentration distribution and head distribution in unconfined coastal aquifer are shown in Figure 14 and 15.

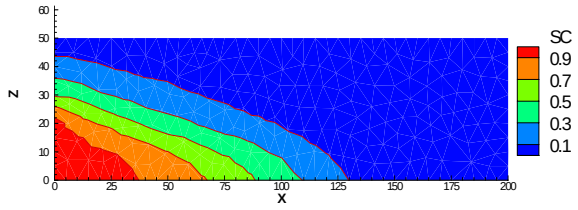

Figure 15: Salt concentration distribution, for steady state, in unconfined coastal aquifer

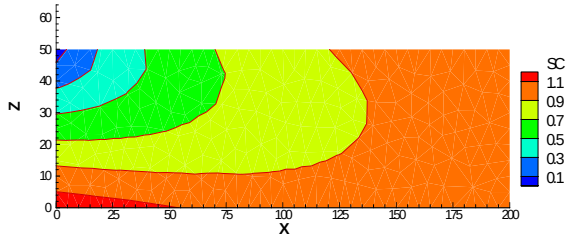

Figure 16: Head distribution, for steady state, in unconfined coastal aquifer

Conclusion

In present work, a 2D numerical model based on finite volume unstructured mesh (FVUM) method is developed for evaluating saltwater intrusion. Presented model solve a flow equation that describes the head distribution in the aquifer of interest and an equation for transport and dispersion of a concentration (i.e. salt). The model solves two equations in a coupled manner explicitly. The model can predict salt concentration distribution in coastal aquifers. In order to verify the model results, Henry's [1959] problem and Huyakorn's [1987] problem solved and results of salt concentration distribution are compared with the results of other researches. Acceptable agreement between the results of the present simulation and previous results are encouraging.

Acknowledgements

The authors sincerely thank Engineering office of water resources project of Tehran Regional Water Board for many discussion and equipment.

References:

[1]- Bear, J., "Hydraulics of Groundwater", McGraw-Hill, New Your, 1979.

[2]-Cheng, J. R., Strobl, R. O., Yeh, G.T., Lin, H.C. and Choi, W. H., "Modeling of 2D density-dependent flow and transport in the subsurface," J. Hydro. Eng., 3(4), 1998, 248-257.

[3]-Frind, E. O., "Simulation of long-term trasient density-dependent transport in groudwater," Adv. Water Resour, 5(2), 1982, 73-88.

[4]-Galeati, G., Gambolati, G., and Neuman, S. P.. "Coupled and partially coupled Eulerian-Lagrangian model of freshwater-seawater mixing." Water Resurces. Res. , 28(1), 1992,149-165.

[5]-Henry, H. R., "Salt intrusion into freshwater aquifers," J. Geophyd. Res., 1959, 64, 19111919.

[6]-Henry, H. R., “Effects of dispersion on salt encroachment in coastal aquifers, in Sea Water in Coastal Aquifers,” (Ed. H. H. Cooper et al.) US Geological Survey Water Supply Paper 1613-C.
[7]-Hoffmann K.A and Chiang S.T, "Computional Fluid Dynamic for Engineers", Engineering Education System, 1993.
[8]-Huyakorn, P. S. Andersen, P. F., Mercer, J.W., and White Jr., H. O., “Saltwater intrusion in aquifers: Develpoment and testing of a three-dimensional finite element model,” Water Resour. Res., 23(2), 1987, 293-312.
[9]-Liu F., Turner I., Anh V., "A Finite Volume Unstructured Mesh Method for Modeling Saltwater Intrusion into Aquifer Systems", First International Conference on Saltwater Intrusion and Coastal Aquifers—Monitoring, Modeling, and Management. Essaouira, Morocco, April 23–25, 2001.
[10]- Ru Y., Jinno K., Hosokawa T. and Nakagawa K., "Study on Effect of Subsurface Dam in Coastal Seawater Intrusion", First International Conference on Saltwater Intrusion and Coastal Aquifers—Monitoring, Modeling, and Management. Essaouira, Morocco, April 23–25, 2001.
[11]- Schwartz F.W and Zhang H., "Fundamentals of Groundwater", John Wiley & Sons, New York, 2003.
[12]-Segol. G., Pinder, G. F. and Gray, W. G. (1975) “A galerkin finite element technique for calculating the transient position of the saltwater front.” Water Res., 11(2), 1975, 343-347.